International Journal of Advanced Technology and Engineering Exploration, Vol 10(105)
ISSN (Print): 2394-5443 ISSN (Online): 2394-7454
http://dx.doi.org/10.19101/IJATEE.2022.10100564

Research Article

Dual-zone control of the traction permanent magnet synchronous motor in the unmanned aerial vehicle

Denis Kotin*, Yuriy Pankrats, Artem Davydov and Ilya Ivanov
Novosibirsk State Technical University, 20 Prospectus K. Marks, Novosibirsk, 630073, Russia

Received: 21-December-2022; Revised: 07-August-2023; Accepted: 08-August-2023

Abstract
The study of the electric drive of unmanned aerial vehicles (UAVs) is relevant in connection with their use in many sectors of the civil industry. However, the study of new designs and controls for single-engine and multi-engine UAVs never stops, as more and more border regions begin to actively use them. The purpose of the modification is to improve the regulatory properties and reduce energy consumption for control. In this work, research, and development of a two-zone electric drive for an UAV of short and medium range, providing a flight range of up to 150 km and having a load capacity of up to 100 kg of a multi-engine type, were carried out. A potential approach for controlling the rotor speed of a permanent magnet synchronous motor (PMSM) was introduced. The study's findings are derived from two scenarios of electric drive operation: the nominal mode and the mode with an elevated rotor speed of the PMSM. Results were presented, indicating the efficiency of the algorithm under high-power conditions. The electric drive for the PMSM with two-zone control increased the speed of the PMSM rotor beyond the nominal value, with minimal losses, while also decreasing the power consumption of the UAV. Theoretical results are confirmed by simulation of a closed system in SimInTech.

Keywords
Unmanned aerial vehicles, Permanent magnet synchronous motor, Mathematical modelling, Frequency converter.

1.Introduction
Unmanned aerial vehicles (UAVs) represent an incredibly exciting story of innovation, closely linked to the development of aeronautics and robotics. Starting with the idea of creating autonomous flying devices, which originated in the middle of the 20th century, this segment has undergone significant development in recent decades, especially at the present time.

In the 1960s, the first experimental prototypes of UAV were created, which were widely used for military and scientific purposes. However, they were cumbersome and required significant human intervention to operate.

In the 1990s, with the development of microelectronics and computer technology, a new era in the development of UAVs began. Miniature and compact drones have become affordable due to improvements in autonomy, sensors and data transfer capabilities. This has led to their wide application in various fields, including environmental monitoring, search and rescue operations, civil aviation and entertainment purposes.

Modernity is characterized by the rapid development of UAVs. The use of advanced technologies such as artificial intelligence, machine learning and computer vision allows the creation of smart and self-learning systems. Commercial companies are increasingly attracted to the UAV industry, offering innovative solutions for the delivery of goods, infrastructure monitoring and other tasks.

The development of UAVs is currently gaining momentum in many civilian industries such as real-time monitoring, remote area communications, remote sensing, terrain mapping, search and rescue, goods delivery and many other areas. However, the study of new designs and controls for single-engine and multi-engine UAVs never stops, as more and more border regions begin to actively use them [1, 2].

The UAV electric drive is a system that is used to control the UAV. It consists of motors, propellers, a

*Author for correspondence

controller and other electronic components that work together to control the direction and speed of the UAV [3].

The main task of the electric drive is to control the motors of the UAV in such a way that they can perform the necessary movements. This can be, for example, taking off, flying at a certain altitude, turning or descending. The drive controller receives information about the current position of the UAV and calculates exactly what actions need to be taken in order to reach the desired destination. It then sends signals to the motors, which change their speed and direction of rotation to perform the required movements. The propellers, which are mounted on the ends of the motors, can also change their direction to help the UAV maintain its desired orientation in space [3, 4].

Depending on the type of UAV and its purpose, the electric drive may be different. For example, for small drones used for photography or videography, electric drive can be relatively simple, consisting of a few motors and a controller. For more complex UAVs or multi-purpose military drones, electric drive may be more complex and consist of more components such as additional sensors, batteries, communication systems, etc.

At present, UAV electric drive is widely used in various fields such as military, commercial and scientific. It plays an important role in the development of unmanned technology and makes a significant contribution to improving the efficiency, safety and accuracy of UAVs [4–6].

Thus, a brushless direct current (DC) motor is often used as an electric drive for the main movement due to the absence of rubbing parts, small dimensions, low cost and ease of control, since most UAVs use a DC power system. However, permanent magnet synchronous motors (PMSM) have high power, reliability, efficiency and controllability over a wide speed range. Also, when using the PMSM in the UAV, it is possible to use two-zone control, which is impossible with a DC motor. The second zone allows you to change the speed of rotation of the rotor when the critical moment of the PMSM changes [3–6]. This article proposes to determine the prospects for the use of two-zone control in UAVs.

For the first time, field-oriented control (FOC) was proposed by Felix Blaschke in 1970, and it consists in the fact that there is a separate control of the torque and the motor flux linkage. Traditionally, two-zone regulation is carried out by weakening the magnetic field in motors with electromagnetic excitation, however, field weakening in PMSM without an additional control channel can be implemented by introducing a demagnetizing armature reaction, that is, introducing current along the d axis, which leads to a weakening of the magnetic field. This will allow, at the same values of current Id, to create an additional magnetic field directed against permanent magnets, that is, it will further weaken the resulting magnetic field and expand the range of speed control(SC) with power constancy, which is the second control zone [7, 8].

Two-zone control can be applied in cases where the propellers of the UAV require a large number of revolutions and while maintaining engine power. Such conditions are observed in a narrow range, however, during a long flight, this control method can reduce power consumption. This article proposes to determine the prospects for the use of two-zone control in UAVs.

Previously, the beginning of the study was presented at the conference [9], this article presents a continuation, which presents a more detailed presentation of the methodology and more accurate results obtained during the work.

This paper aims to compare the operation of PMSM in power up and decoupling modes. Moreover, section 2 discusses the literature that the authors used to obtain the necessary, additional information. Section 3 is a discussion of the methods, approaches, and principles that the authors used to develop the model. Section 4 presents the results obtained during the simulation. Section 5 is the discussion of the results, and section 6 concludes this work.

2.Literature review

The topic of optimizing the energy consumed in UAVs is of interest to many authors, where everyone tries to contribute. Here, for example, in [10], the authors conduct a similar study, where they propose a control strategy for an internal permanent magnet synchronous motor (IPMSM) based on model predictive control (MPC).

In articles [1, 2], the authors explore the use of UAVs in the civil sphere and highlight key research challenges. They look at different UAV applications such as surveying, cartography, rescue operations and

transportation, and discuss key issues such as safety, legislation and efficiency.

In [4], the authors analyze the influence of system components, such as a battery, voltage regulator, and charge control devices, on the efficiency of a UAV. The authors also evaluate the performance of the system and draw conclusions about its applicability for solving practical problems.

Also, in many articles, the authors solve the problems of energy efficiency, increasing the torque or increasing the speed of PMSM, such as in [8, 11–16]. Thus, in [8], the authors propose to change the classical FOC by introducing an additional parameter, which reduces the load on the computing unit, which, as a result, can lead to the elimination of unnecessary energy costs in the UAV, or in [16], motor torque control is the key, which, when implemented in UAV, can lead to energy efficiency, but the developed algorithm requires high computing power, which will require additional energy costs.

First, the authors perform mathematical modeling of IPMSM and use it to develop the MPC algorithm for high – speed operation. The proposed MPC-based flux reduction control strategy takes into account various constraints such as torque, current and voltage, and provides optimal control parameters for maximum motor efficiency.

From the above works, it can be seen that research in the field of energy consumption optimization in UAVs is being actively carried out, and the authors are looking for various approaches to improve the efficiency of engines and systems. However, some of the proposed solutions may be limited by the size of the system, which leads to additional energy costs, such as [1, 2, 4], and in the article [13], the proposed solution for an electric drive requires high-performance computing systems that consume a large amount of energy.

3.Methods

Development of a UAV thrust drive control system

To implement the second control zone, it is required to weaken the motor flux linkage, as a result of which the maximum torque will decrease, and the speed will become higher. However, the power will remain unchanged. The graph of this transition is illustration in *Figure 1*.

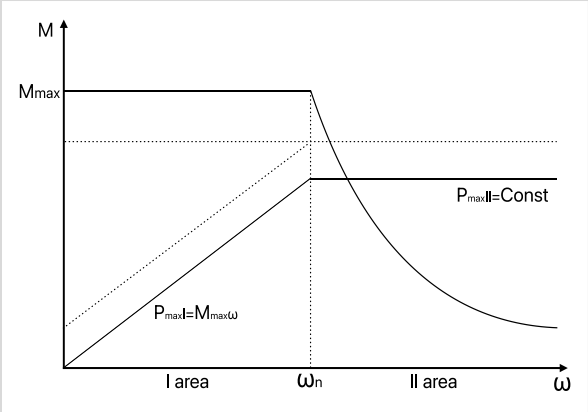

Figure 1 Diagram of the transition PMSM to the second control area

The structure of the UAV electric traction drive is shown in *Figure 2* and has a generally accepted structure, it is a control controller, an inverter, a DC voltage source, and PMSM is also used.

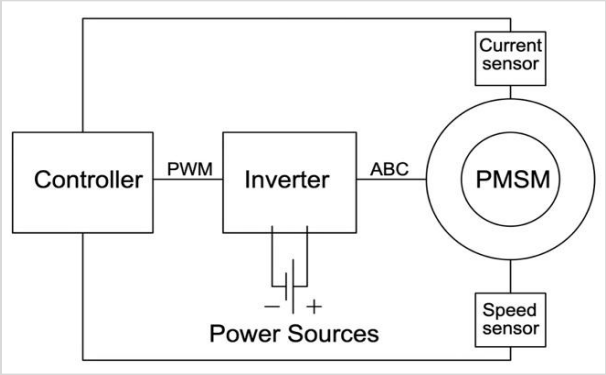

Figure 2 Structural diagram of the electric drive

The dq system was chosen as the coordinate system and the block diagrams of the electric drive along the current q and current d axes were drawn up separately. Block diagrams are illustration in *Figure 3* and *Figure 4.*

To move to the second control zone, it is required to weaken the flow; for this, a flux linkage controller was added on the current axis d in the circuit

Figure 3 is a diagram that represents the actions of the control system in the current q-axis, while *Figure 4* shows the control of the system along the current d-axis. Both control samples are focused on one of the motors, the essence of which lies in the UAV drive mechanism. The details of the diagram in *Figure 3* are from left to right: setting the desired motor speed, final speed feedback, SC, current loop, load control

system, and final speed. The diagram in *Figure 4* is built in the same vein, from left to right: input of the desired motor speed, final speed feedback, SC, flux feedback, flux controller, load control system, and finally the final speed [11, 12].

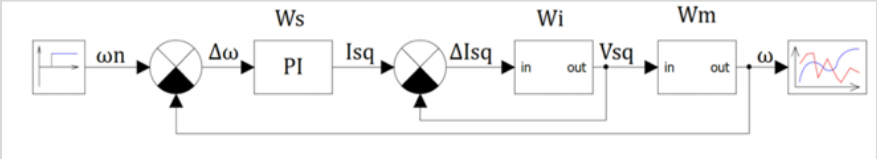

Figure 3 Structural diagram of the electric drive along the current axis q

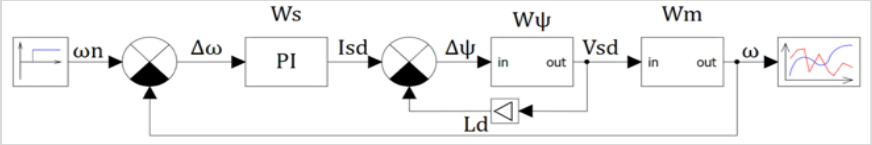

Figure 4 Structural diagram of the electric drive along the current axis d

PMSM is described by the formulas (Equation 1):

$$\begin{cases} pI_{Sd} = \frac{1}{L_{Sd}}(U_{Sd} - R_s I_{Sd} + \omega_e L_{Sq} I_{Sq}) \\ pI_{Sq} = \frac{1}{L_{Sq}}(U_{Sq} - R_s I_{Sq} + \omega_e L_{Sd} I_{Sd} - \psi_f \omega_e) \\ M_{em} = \frac{3Z_p}{2}(I_{Sq}\Psi_f + I_{Sd} I_{Sq}(L_{Sd} - L_{Sq})) \end{cases} \quad (1)$$

The proportional integral (PI) current controller (CI) is calculated according to the formula (Equation 2):

$$U_d = k_p e + k_i \int e dt \quad (2)$$

where: k_p – calculated proportional link; k_i – calculated integral link

Derived closed system formula for the link k_p as shown in Equation 3.

$$k_p = \frac{k_1 \cdot \frac{L}{r}}{(a_1 \cdot \frac{1}{r} \cdot \frac{U}{U_n})} \quad (3)$$

where: k_1 – current feedback; a_1 – selected coefficient

Derived closed system formula for the link k_i as shown in Equation 4.

$$k_i = \frac{k_1}{(a_1 \cdot \frac{1}{r} \cdot \frac{U}{U_n})} \quad (4)$$

The proportional differential (PD) speed controller is calculated according to the formula (Equation 5):

$$U_d = k_p e + k_d \frac{de}{dt} \quad (5)$$

Derived closed system formula for the link k_p as shown in Equation 6.

$$k_p = \frac{k_1 \cdot k_2 \cdot J}{(a_2 \cdot W_m)} \quad (6)$$

where: k_2 – speed feedback; a_2 – selected coefficient

Derived closed system formula for the link k_d as shown in Equation 7.

$$k_d = \frac{a_1 \cdot k_2 \cdot J}{(a_2 \cdot W_m \cdot k_1)} \quad (7)$$

I/U transfer function for machine (Equation 8):

$$W_i = W_{ci} \cdot k \cdot W_{co} \quad (8)$$

where: W_{ci} – is the transfer function of the CI
k – coefficient of the converter
W_{co} – is the transfer function of the control object (CO)

The transfer function of forming the moment on the machine shaft is identical for the circuit q and d, and has the form as shown in Equation 9.

$$W_m = \frac{3}{2} \cdot Z_p \cdot \Psi \cdot \frac{1}{J \cdot s} \quad (9)$$

where: Z_p – is the number of pole pairs
Ψ – flux linkage of the rotor of the machine
J – is the moment of inertia of the motor
The speed loop transfer function for current q in *Figure 2* is shown as in Equation 10.

$$W_s = W_{sc} \cdot W_i \cdot W_m \quad (10)$$

where: W_s – is the transfer function of the speed loop
W_{sc} – transfer function of the speed controller
W_i – is the transfer function of the current loop
W_m – is the transfer function of the motor torque

The transfer function of the speed loop for current d in *Figure 3* is distinguished by the presence of a flux linkage controller (Equation 11).

$$W_S = W_{sc} \cdot W_\psi \cdot W_m \quad (11)$$

where: W_ψ – is the transfer function of the flux linkage loop

Transfer function of the flux linkage circuit for current d in *Figure 3* (Equation 12).

$$W_\psi = \frac{L_d \cdot W_{c\psi} \cdot W_i}{1 + L_d \cdot W_{c\psi} \cdot W_i} \quad (12)$$

where: Control Linkage ($W_{c\psi}$) – is the transfer function of the flux linkage controller

L_d – is the stator inductance along the current loop d

To weaken the flux linkage, a flux linkage control unit (Rψ) is introduced into the classic two-loop FOC system [7, 8].

The mathematical model of the PMSM control system in dq coordinates is illustration in *Figure 5* [8–10]. From the PMSM mathematical model, we obtain the diagrams is illustration in *Figure 6* and *7*.

Figure 6 shows a diagram of PMSM operation in nominal mode. The diagrams contain vectors: E_g - General, electromotive force (EMF), E_q - EMF along the q axis, E_{qr} - EMF along the q axis rated, E_d - EMF along the d axis, E_s - EMF module, E_{sr} - EMF rated module, I_q - current along the q axis, I_d is the current along the d axis, I_s is the current modulus, $L_qI_q\omega$ is the EMF of the rotor response along the q axis, $L_dI_d\omega$ is the EMF vector of the rotor response along the d axis. As can be seen in the diagram in *Figure 7*, in the case of $M < M_{in}(\omega)$, the value of $L_qI_q\omega$ decreases, in this mode, the inverter is not fully used in terms of voltage. Such use is not rational since it requires an overestimated value of I_d. In this case, I_d can be reduced to provide the mode shown in *Figure 8*.

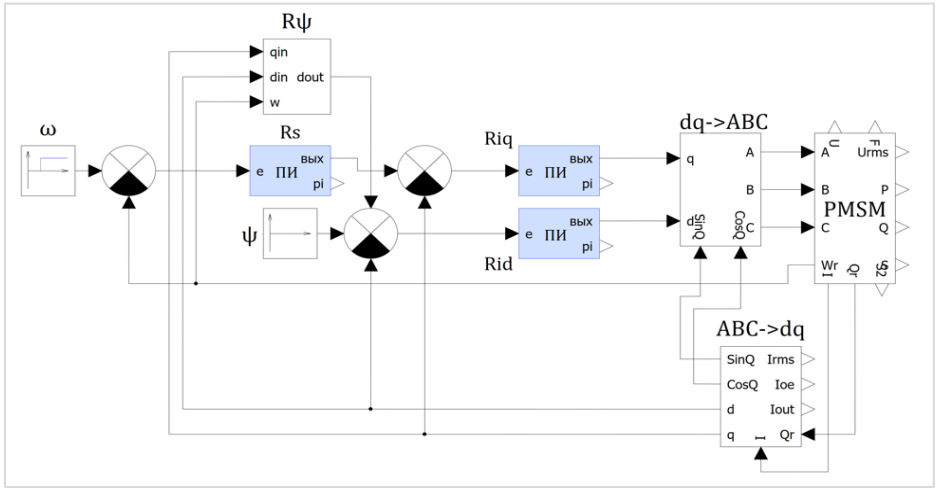

Figure 5 Mathematical model of the PMSM control system

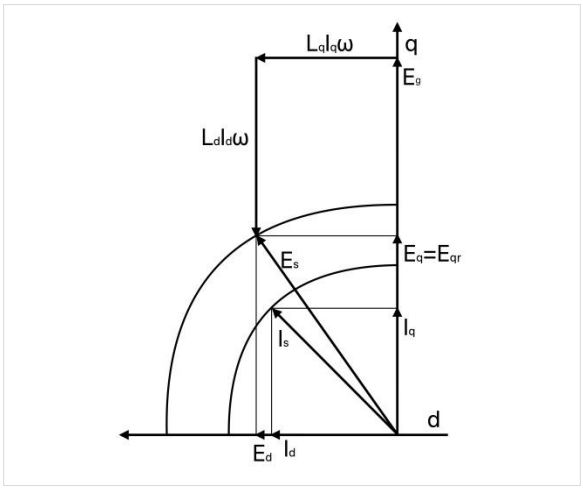

Figure 6 Diagram of PMSM work in the first zone

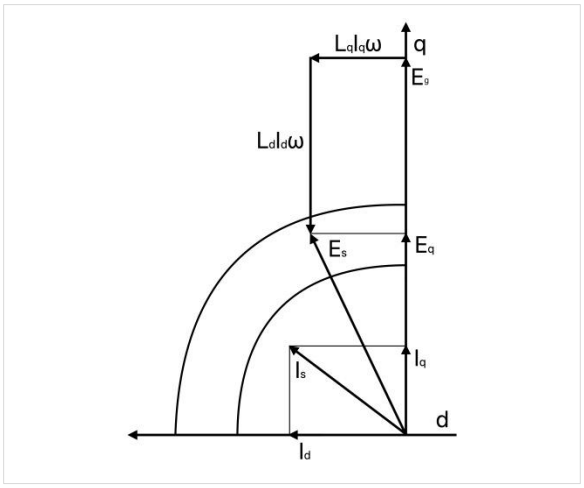

Figure 7 Scheme of PMSM with reduced M

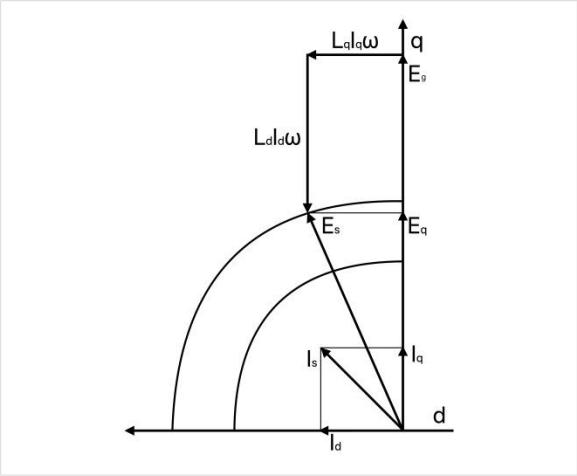

Figure 8 Diagram of PMSM work in the second zone

To work according to the algorithm that ensures operation according to the diagram shown in *Figure 8*, that is, providing $E_s = E_{sr}$ at $M(\omega) \le M_{in}(\omega)$, it is necessary to provide a functional the dependence of the longitudinal current I_d not only on ω, but also on I_q (Equation 13).

$$I_d = \frac{E_q - E_g}{L_d \cdot \omega \cdot p_{in}} = \frac{\sqrt{E_{sr}^2 - \left(L_q i_q \omega P_{in}\right)^2} - C\Phi_f \omega P_{in}}{L_d \cdot \omega \cdot p_{in}} \quad (13)$$

This algorithm allows, with limited EMF rotation, to achieve higher rotor speeds. This will allow, at the same values of current I_d, to create an additional magnetic field directed against permanent magnets, which will weaken the resulting field and expand the range of SC with power constancy.

The mathematical model is aimed at calculating the possibility of controlling the corresponding engines in the second zone of the UAV. The analysis of the second zone becomes important, since the regulation of the motor flux linkage affects cosφ, which, while maintaining the motor power, contributes to an increase in the rotor speed while reducing the critical moment of the electric motor. For UAVs, this brings the advantage of increased energy efficiency, which has a positive effect on flight duration [3, 5–11].

4.Results

For simulation, the engine parameters indicated in *Table 1* were used, all calculations were performed in the SimInTech mathematical modeling environment. Models of PMSM, PI-controllers verified by software developers SimInTech.

Table 1 Characteristics of PMSM

S. No.	Motor characteristics	Standard value
1	Pole number	4
2	Rated output	2200 W
3	Voltage	360 V
4	Rated speed	1500 rpm
5	Rated frequency	50 Hz
6	Efficiency η	90.5%
7	Rated current	6 A
8	Torque	14 Nm
9	Max. Torque (2 min)	45Nm
10	Power factor	0.99η
11	Phase resistance	2.1 Ω

In the bottom mathematical model, a calculation was made to increase the rotor speed by 1.5 times.

Figure 9 shows a graphical representation of the motor speed, illustrating the following steps: initiation of the motor start, operating mode at standard speed, transition to high speed, and steady state at high speed. It takes 0.1 seconds for the engine to accelerate to rated speed, and 0.25 seconds from the start of the upshift until a steady state of high speed is reached.

Figure 10 is a plot of the current in the dq coordinate system. It can be seen from the graph that the current in the nominal mode tends to zero due to the moment of resistance equal to 1, and when switching to an increased speed, the current along the d axis increases, which leads to a weakening of the stator magnetic field. It should be noted that the total motor current does not exceed the motor rated current. Based on the data obtained, it can be seen that at an increased speed the engine consumes no more power than in the nominal mode, and this is achieved by changing the flux linkage. To increase the rotational speed by increasing the power, it is necessary to apply more current to the motor. *Figure 11* shows the current graph during the transition to the second zone due to an increase in engine power.

Figure 11 shows that the average current value increases by 7-8 times with an increase in speed, which under conditions of rated loads can be equal to 32-36A, with a rated current value of 4.5A. With a short-term change, such an excess of current will not lead to negative consequences for the motor, however, the energy consumption significantly exceeds those that will be necessary with the proposed two-zone control.

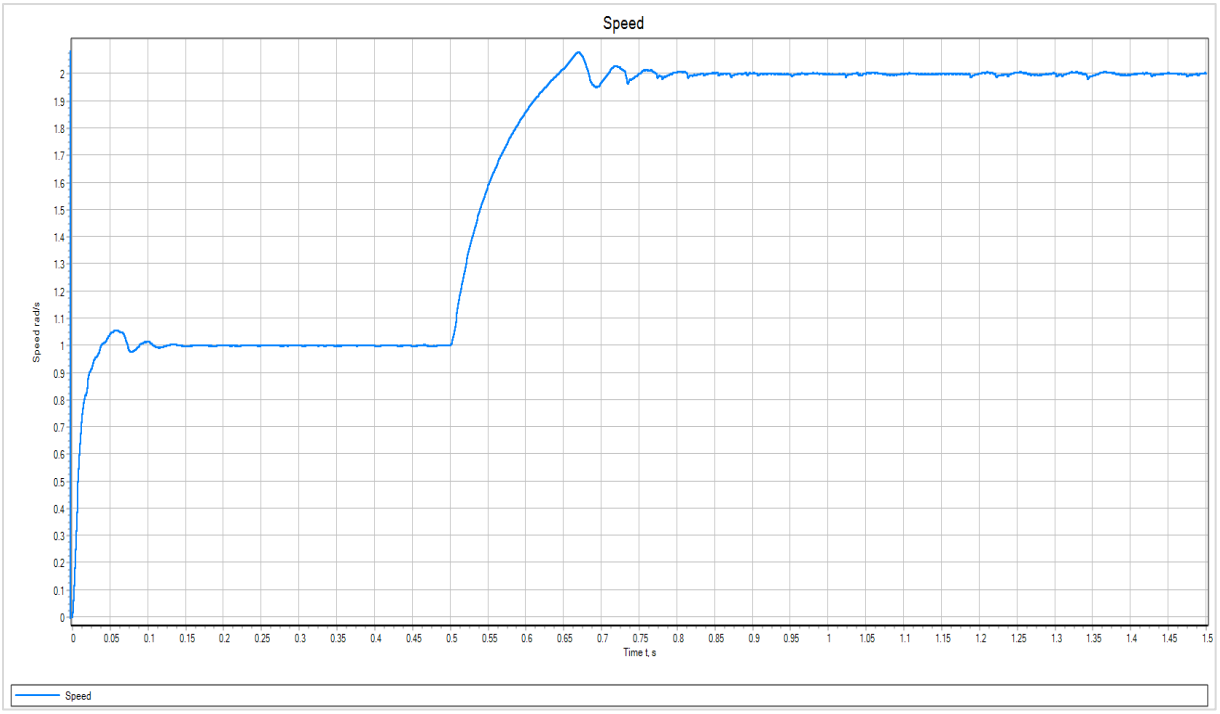

Figure 9 Graph of speed, rad/s

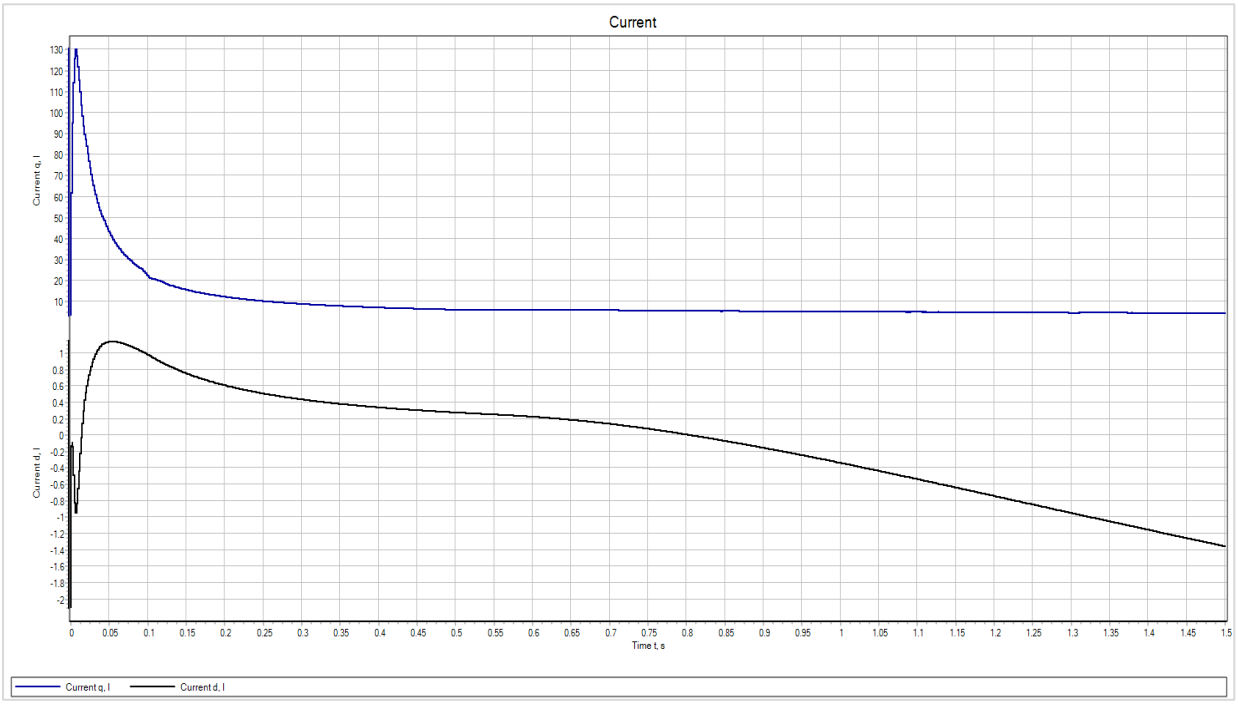

Figure 10 Current graph, I in the coordinate system dq

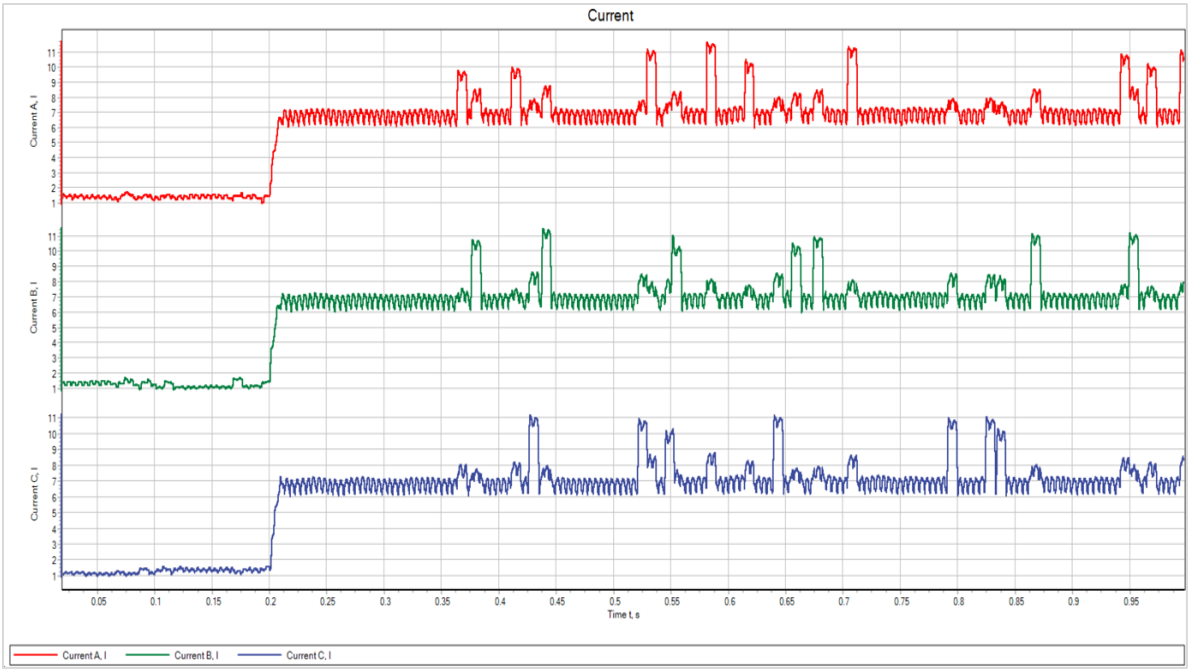

Figure 11 Current graph, I in the coordinate system abc

5.Discussion

This article studies a promising two-zone algorithm for controlling the electric drive of synchronous motors with permanent magnets in UAVs. In the course of the study, mathematical modeling of an electric drive with PMSM was carried out, as a result of which the following results were obtained: when the flux linkage is weakened, the motor can reach a speed 1.5 times higher than the nominal one, with a decrease in the maximum torque, as a result of which the power of the electric drive does not change, which leads to improved energy efficiency up to 8 times than with a conventional increase in speed by 1.5 times due to increased power. This can improve the energy efficiency of using the UAV control system in practice. However, the proposed algorithm can work in a narrow range of speed increase, for example, with a headwind gust, however, in such situations, this can save additional electricity, as well as increase the reliability of the device, due to the fact that the current consumed will not exceed the nominal values, which means that all circuit elements will work in normal mode. Also, the acceleration of the electric motor by more than two times can lead to self-destruction if the mechanical part of the electric motor is not modernized. Due to the high cost of the PMSM, it was decided to preliminarily conduct a mathematical modeling of the control system, and in case of positive results, proceed to bench tests. In the presented mathematical model of the PMSM, all models are ideal, and therefore, the real results may differ. In future articles on this topic, it is planned to present the results of bench simulation on a real PMSM, where it will be possible to compare the results obtained by the simulation method and the results obtained from the real model.

A complete list of abbreviations is shown in *Appendix I.*

6.Conclusion

The PMSM control system is a key element of the electric drive of UAVs. To control the PMSM engine, mathematical modeling was performed, which made it possible to evaluate its operation at nominal and increased speeds. The simulation results showed that when controlling the PMSM in the second speed zone, the power consumption of the control system does not exceed the nominal values. Thus, the developed PMSM control system provides effective control of the electric drive of UAVs, which, in turn, ensures their reliable and safe operation. This will increase the energy efficiency of UAV use in practice.

Acknowledgment

None.

Conflicts of interest

The authors have no conflicts of interest to declare.

Author's contribution statement

Denis Kotin: Study conception, design, supervision, investigation on challenges. **Yuriy Pankrats:** Study conception, data collection, supervision, investigation on challenges. **Artem Davydov:** Conceptualization, investigation, data collection, writing – original draft, writing – review and editing. **Ilya Ivanov:** Study conception, data collection, supervision, investigation on challenges and draft manuscript preparation.

References

[1] Song Z, Zhang H, Zhang X, Zhang F. Unmanned aerial vehicle coverage path planning algorithm based on cellular automata. In 15th international conference on computational intelligence and security 2019 (pp. 123-6). IEEE.

[2] Shakhatreh H, Sawalmeh AH, Al-fuqaha A, Dou Z, Almaita E, Khalil I, et al. Unmanned aerial vehicles (UAVs): a survey on civil applications and key research challenges. IEEE Access. 2019; 7:48572-634.

[3] Lee SG, Bae J, Kim WH. A study on the maximum flux linkage and the goodness factor for the spoke-type PMSM. IEEE Transactions on Applied Superconductivity. 2017; 28(3):1-5.

[4] He X, Sun X, Wang F, Li X, Zhuo F, Luo S. Design of energy management system for a small solar-powered unmanned aerial vehicle. In 9th IEEE international symposium on power electronics for distributed generation systems 2018 (pp. 1-4). IEEE.

[5] Xu X, Novotny DW. Selection of the flux reference for induction machine drives in the field weakening region. IEEE Transactions on Industry Applications. 1992; 28(6):1353-8.

[6] Joshi D, Deb D, Muyeen SM. Comprehensive review on electric propulsion system of unmanned aerial vehicles. Frontiers in Energy Research. 2022; 10:1-20.

[7] Carpaneto M, Marchesoni M, Vallini G. Practical implementation of a sensorless field oriented PMSM drive with output AC filter. In SPEEDAM 2010 (pp. 318-23). IEEE.

[8] Kolano K. New method of vector control in PMSM motors. IEEE Access. 2023; 11: 43882-90.

[9] Davydov A, Pankrats Y, Ivanov I, Bayanov E, Chipurnov S. Analysis of the application of traction engines in unmanned aerial vehicles. In electrical complexes and systems 2022 (pp. 235-43). UFA.

[10] Zhang Y, Qi R. Flux-weakening drive for IPMSM based on model predictive control. Energies. 2022; 15(7):1-14.

[11] Davydov A, Bochenkov B, Anosov V. Compact inverter for single-phase induction motor. In international Russian automation conference 2021 (pp. 74-8). IEEE.

[12] Yu Y, Cong L, Tian X, Mi Z, Li Y, Fan Z, et al. A stator current vector orientation based multi-objective integrative suppressions of flexible load vibration and torque ripple for PMSM considering electrical loss. CES Transactions on Electrical Machines and Systems. 2020; 4(3):161-71.

[13] Chau KT, Chan CC, Liu C. Overview of permanent-magnet brushless drives for electric and hybrid electric vehicles. IEEE Transactions on Industrial Electronics. 2008; 55(6):2246-57.

[14] Schauder C. Adaptive speed identification for vector control of induction motors without rotational transducers. In conference record of the industry applications society annual meeting, 1989 (pp. 493-9). IEEE.

[15] Zhang Y, Huang L, Xu D, Liu J, Jin J. Performance evaluation of two-vector-based model predictive current control of PMSM drives. Chinese Journal of Electrical Engineering. 2018; 4(2):65-81.

[16] Huang MS, Chen KC, Chen CH, Li ZF, Hung SW. Torque control in constant power region for IPMSM under six-step voltage operation. IET Electric Power Applications. 2019; 13(2):181-9.

Denis Kotin was born in Novosibirsk, Russia, in 1984. He earned his B.S., M.S., and Cand. of Tech. Sc. degrees in electrical engineering from Novosibirsk State Technical University, Russia, in 2005, 2007, and 2010, respectively. He presently serves as the Head of the Department of Electric Drive and Industry Automation at Novosibirsk State Technical University. His research interests primarily encompass the automatic control of AC electric drives and power electronic devices.
Email: d.kotin@corp.nstu.ru

Yuriy Pankrats, was born in the Novosibirsk region, Russia, in 1979. He earned the title of electromechanical engineer in 2007. In 2011, he attained his Cand. of Tech. Sc. degree from Novosibirsk State Technical University, Russia. Presently, he holds the position of engineer at the scientific research laboratory "Testing of Electric Drive," which falls under the purview of the Department of Electric Drive and Industry Automation at Novosibirsk State Technical University. His research interests encompass automatic control of AC electric drives and power electronic devices, along with the testing of electric generators and drones.
Email: pankracz@corp.nstu.ru

Artem Davydov was born in Barnaul, Russia, in 1996. He obtained his B.S. and M.S. degrees in electrical engineering from Polzunov Altay State Technical University, Russia, in 2018 and 2020, respectively. At present, he is a postgraduate student within the Department of Electric Drive and Industry Automation at Novosibirsk State Technical University. His research interests primarily lie in the field of Automatic Control of Electric Drives and Power Electronic Devices.
Email: nobody.one911@icloud.com

Ilya Ivanov was born in Barnaul, Russia, in 1995. He obtained his B.S. and M.S. degrees in electrical engineering from Polzunov Altay State Technical University, Russia, in 2018 and 2020, respectively. Currently, he is a postgraduate student in the Department of Electric Drive and Industry Automation at Novosibirsk State Technical University. His research interests encompass Automatic Control of Electric Drives and Power Electronic Devices.
Email: i.a.ivanov@corp.nstu.ru

Appendix I

S. No.	Abbreviation	Description
1	Cψ	Control Linkage
2	CO	Control Object
3	CI	Current Controller
4	DC	Direct Current
5	EMF	Electromotive Force
6	FOC	Field-Oriented Control
7	IPMSM	Internal Permanent Magnet Synchronous motor
8	MPC	Model Predictive Control
9	PMSM	Permanent Magnet Synchronous Motor
10	PD	Proportional Differential
11	PI	Proportional Integral
12	SC	Speed Control
13	UAVs	Unmanned Aerial Vehicles